

1 **TITLE PAGE**

2 Running head: Integrated spatial models

3 **Title: Integrated spatial models foster complementarity between monitoring**
4 **programs in producing large-scale bottlenose dolphin indicators**

5

6 **Authors:** Valentin Lauret¹, Hélène Labach^{2,1}, Daniel Turek³, Sophie Laran⁴,
7 Olivier Gimenez¹

8

9 (1) CEFE, Université Montpellier, CNRS, EPHE, IRD, Montpellier, France

10 (2) MIRACETI, Connaissance et conservation des cétacés, Place des traceurs de pierres,
11 13500 La Couronne, France

12 (3) Williams College, Department of Mathematics & Statistics, Williamstown, MA 01267,
13 USA, dbt1@williams.edu

14 (4) Observatoire PELAGIS, UMS 3462 CNRS-La Rochelle Université, 5 allée de l’Océan,
15 17000 La Rochelle

16

17

18 **Mailing address of the authors**

19

20 Valentin Lauret: valentin.lauret@ens-lyon.fr

21 Hélène Labach: hlabach@miraceti.org

22 Daniel Turek: dbt1@williams.edu

23 Sophie Laran: sophie.laran@univ-lr.fr

24 Olivier Gimenez: olivier.gimenez@cefe.cnrs.fr

25

26 Corresponding author: Valentin Lauret, valentin.lauret@ens-lyon.fr, CEFE 1919 Route de
27 Mende, 34090 Montpellier, France.

28

29

30 **Article: Integrated spatial models foster complementarity between
31 monitoring programs in producing large-scale bottlenose dolphin indicators**

32 **Abstract (< 300 words)**

33 Over the last decades, large-scale ecological projects have emerged that require
34 collecting ecological data over broad spatial and temporal coverage. Yet, obtaining relevant
35 information about large-scale population dynamics from a single monitoring program is
36 challenging, and often several sources of data, possibly heterogeneous, need to be integrated.
37 In this context, integrated models combine multiple data types into a single analysis to quantify
38 population dynamics of a targeted population. When working at large geographical scales,
39 integrated spatial models have the potential to produce spatialised ecological estimates that
40 would be difficult to obtain if data were analysed separately.

41 In this paper, we illustrate how spatial integrated modelling offers a relevant framework
42 for conducting ecological inference at large scales. Focusing on the Mediterranean bottlenose
43 dolphins (*Tursiops truncatus*), we combined 21,464 km of photo-identification boat surveys
44 collecting spatial capture-recapture data with 24,624 km of aerial line-transect following a
45 distance-sampling protocol. We analysed spatial capture-recapture data together with distance-
46 sampling data to estimate abundance and density of bottlenose dolphins. We compared the
47 performances of the distance sampling model and the spatial capture-recapture model fitted
48 independently, to our integrated spatial model.

49 The outputs of our spatial integrated models inform bottlenose dolphin ecological status
50 in the French Mediterranean Sea and provide ecological indicators that are required for regional
51 scale ecological assessments like the EU Marine Strategy Framework Directive. We argue that
52 integrated spatial models are widely applicable and relevant to conservation research and
53 biodiversity assessment at large spatial scales.

54 **Keywords**

55 *Bottlenose dolphins, data integration, distance sampling, integrated models, Marine Strategy*

56 *Framework Directive, NIMBLE, spatial capture-recapture*

57 **Introduction**

58 Macro-institutions get increasingly involved in large-scale programs for biodiversity
59 conservation over regional and continental areas. Whether these policies aim at assisting
60 governments (e.g., the Intergovernmental Science-Policy Platform on Biodiversity and
61 Ecosystem Services), or at implementing environmental management such as the European
62 Union directives (Habitat Directive, 92/43/EEC, or Marine Strategy Framework Directive,
63 MSFD, 2008/56/EC), conducting large-scale ecological monitoring is required to establish
64 conservation status of targeted species and ecosystems, and to inform decision-making.

65 For biodiversity management decisions, conservation sciences require assessing the
66 ecological status of species and ecosystems, which democratized the call for ecological
67 indicators (Buckland, Magurran, et al., 2005; Nichols & Williams, 2006). An ecological
68 indicator can be defined as a metric reflecting one or more components of the state of ecological
69 systems. An ecological indicator can either be measured directly or result from the
70 simplification of several field-estimated values (Niemi & McDonald, 2004). The Marine
71 Strategy Framework Directive referred to abundance/density of targeted species (e.g. seabirds,
72 cetaceans) as ecological indicators to fulfil for national reporting. At large spatial scales,
73 logistical and financial constraints often prevent a detailed coverage of the targeted population
74 using a single collection effort, and different monitoring programs coexist (Lindenmayer &
75 Likens, 2010; Zipkin & Saunders, 2018; Isaac et al., 2019). The multiplication of monitoring
76 programs over the same conservation context has fostered the development of statistical models
77 that can estimate ecological quantities while accommodating several, possibly heterogeneous,
78 datasets (Besbeas et al., 2002; Miller et al., 2019; Isaac et al., 2019; Zipkin, Inouye, &
79 Beissinger, 2019; Farr et al., 2020). Integrating data from several monitoring protocols can give

80 complementary insights on population structure and dynamics (Schaub & Abadi, 2011),
81 increase space and time coverage of the population (Schaub & Abadi, 2011; Zipkin, Inouye, &
82 Beissinger, 2019), and produce more precise ecological estimates (Isaac et al. 2019; Lauret et
83 al. 2021; Farr et al. 2020).

84 A recurrent objective of ecological monitoring programs is to estimate population
85 abundance and density (Williams, Nichols, & Conroy, 2002), for which distance sampling (DS,
86 Buckland et al., 2005) and capture-recapture (CR, Williams et al. 2002) methods are widely
87 used. Abundance reflects the estimated number of animals in a specified area while density is
88 a spatialised estimate that reflects the number of animals per unit area. DS and CR methods
89 have strengths and weaknesses in relation to logistical and practical issues (Hammond et al.,
90 2021). DS methods can cover large areas at a reasonable cost (e.g. line transect monitoring),
91 while CR monitoring programs can be costly to develop at large spatial scales because more
92 sampling effort is required over a longer time period to recapture individuals (Hammond et al.,
93 2021). Even when estimating abundance over the same study area, DS and CR do not estimate
94 exactly the same quantity (Calambokidis & Barlow, 2004; Crum, Neyman, & Gowan, 2021).
95 DS methods estimate abundance within a study area at the time of the survey. CR methods are
96 based on individuals sampling and estimate the number of animals that were present in the
97 study area during the time of the monitoring (Calambokidis & Barlow, 2004). CR methods
98 encapsulate longer temporal extent because multiple sampling occasions are needed to build
99 CR histories (Williams, Nichols, & Conroy, 2002). However, when data are collected over the
100 same monitoring period and if animals do not move in and out of the study area during that
101 period, CR and DS provide consistent estimates. Recent modelling tools have emerged to
102 integrate both DS and CR methods into integrated population models (Kéry & Royle 2020). DS
103 and spatial CR methods (SCR) allows accounting for spatial variation in abundance and density
104 (Camp et al., 2020; Miller et al., 2013; Royle et al., 2014), possibly at large scales (Bischof et

105 al., 2020). The extension to integrated spatial models has been proposed to account for spatial
106 variation in abundance and demographic parameters while analysing jointly DS data and SCR
107 data (Chandler et al., 2018). Integrated modelling holds promise for species occurring over
108 large areas that are likely to be the target of multiple monitoring protocols. Besides, working at
109 large geographical scales requires encapsulating spatial dimensions in the estimation of
110 ecological quantities. Integrated spatial models allow to assess spatialised ecological inference,
111 e.g density of individuals. To date, integrated spatial models have been developed and used on
112 open populations to estimate temporal variation in population dynamics and vital rates such as
113 survival and recruitment (Chandler & Clark, 2014; Chandler et al., 2018; Sun, Royle, & Fuller,
114 2019). These applications rely on long-term datasets that are not always compatible with
115 conservation objectives. In many cases, ecological information is needed quickly, and data to
116 investigate temporal variation are unavailable (Nichols & Williams, 2006; Lindenmayer &
117 Likens, 2010). Consequently, ecological inference is often restricted to closed-population
118 indicators (e.g. abundance or population size, density or spatial repartition of the population,
119 distribution or spatial extent of a population). When the temporal resolution of monitoring
120 programs does not allow to quantify population dynamics, we argue that an application of
121 integrated spatial models to closed populations can be useful in numerous ecological contexts
122 to deal jointly with existing monitoring programs and assess abundance and density.

123 In this paper, we build an integrated spatial model and demonstrate the relevance of
124 combining DS and SCR to build large-scale ecological indicators. We consider the monitoring
125 of common bottlenose dolphins (*Tursiops truncatus*) that are considered as “vulnerable” by the
126 IUCN Red List in the North-Western Mediterranean Sea (IUCN, 2009). The protected status of
127 bottlenose dolphins within the French seas (listed on Annex II of the European Habitats
128 Directive) led to the development of specific programs to monitor Mediterranean bottlenose
129 dolphins within the implementation of the European Marine Strategy Framework Directive,

130 which requires assessing the conservation status of this species every 6 years over the large
131 extent of the French Mediterranean Sea (Authier et al. 2017). Increasing efforts are dedicated
132 to develop monitoring programs in the Marine Protected Areas (MPA) network that mainly
133 implement photo-identification protocols locally, while governmental agencies perform large-
134 scale line-transect programs to monitor marine megafauna and fisheries. Hence, multiple data
135 sources coexist about bottlenose dolphins in the French Mediterranean Sea. In this paper, we
136 analysed DS data collected by aerial line-transect surveys over a large area covering coastal
137 and pelagic seas (Laran et al., 2017), which we combined with SCR data collected by a photo-
138 identification monitoring program restricted to coastal waters (Labach et al., 2021). We
139 compared the abundance and density of bottlenose dolphins estimated from DS model, SCR
140 model, and integrated spatial models to highlight the benefits of the integrated approach in an
141 applied ecological situation. We discussed the promising opportunities of using integrated
142 spatial models in the context of marine monitoring planning in the French Mediterranean.
143 Eventually, we underlined the conservation implications of using such a model at a wider extent
144 to make the best use of available datasets.

145 **Methods**

146 **Monitoring bottlenose dolphins in the French Mediterranean Sea**

147 Common bottlenose dolphins (*Tursiops truncatus*) occur over large areas throughout the
148 Mediterranean Sea. Because monitoring elusive species in the marine realm is complex,
149 multiple monitoring initiative have emerged to collect data about bottlenose dolphins in the
150 French Mediterranean Sea. In the context of the Marine Strategy Framework Directive, the
151 French government implemented large-scale aerial transects to monitor marine megafauna
152 (Laran et al., 2017). However, the large spatial coverage of the aerial monitoring is impaired
153 by the low resolution of such data (i.e. 1 campaign every 6 years). Then, to collect detailed data,
154 the French agency for biodiversity funded a photo-identification monitoring program to

155 investigate the ecological status of the bottlenose dolphins in the French Mediterranean Sea.
156 This coastal boat photo-identification monitoring has been performed between 2013 and 2015.
157 Coastal photo-identification monitoring represents a promising opportunity to produce high
158 resolution information because data can be collected routinely by Marine Protected Areas at
159 high time frequency.

160 **Study area and datasets**

161 We focused on an area of 255,000 km² covering the North-Western Mediterranean Sea
162 within which we considered two monitoring programs about bottlenose dolphins. We used SCR
163 data from at-sea boat surveys over 21,464 km of the French continental shelf. Observers
164 performed monitoring aboard small boats to locate and photo-identify bottlenose dolphins all
165 year long between 2013 and 2015, always at constant speed and with three observers. Taking
166 pictures of the dorsal fin of each individual in the group makes possible the construction of
167 detection history and hence the analysis of the population through capture-recapture methods
168 (Labach et al., 2021). Boat surveys were restricted to the coastal waters of France and adopted
169 a search-encounter design covering approximatively all the continental shelf every 3 months.
170 We divided the duration of the monitoring programs into 8 equal sampling occasions that length
171 for 3 months each, following previous analysis by [Labach et al. \(2021\)](#). We also used DS data
172 that were collected during winter and summer aerial line-transect surveys covering 24,624 km
173 of both coastal and pelagic NW Mediterranean Sea between November 2011 to February 2012
174 and May to August 2012 (Laran et al., 2017). Two trained observers collected cetacean data
175 following a DS protocol (i.e. recording species identification, group size, declination angle).
176 Aerial surveys were conditional on a good weather forecast.
177 We divided the study area in 4356 contiguous grid-cells creating a 5'x5' Mardsen grid (WGS
178 84). To model density of individuals, we used depth as an environmental covariate, which is
179 expected to have a positive effect on bottlenose dolphins' occurrence (Bearzi, Fortuna, &

180 Reeves, 2009; Labach et al., 2021). To estimate the sampling effort of aerial and boat surveys,
181 we calculated the transect length (in km) prospected by each monitoring protocol within each
182 grid-cell during a time period. Typically, entire transects are split into segments as they overlap
183 multiple grid-cells (Miller et al., 2013). Sampling effort was therefore cell and occasion-specific
184 in the case of the SCR model, and cell specific for the DS model. Sampling effort ranged from
185 0.047 km to 308 km per grid-cell and per occasion for the photo-id dataset, and from 1.33 to
186 54560 km per grid-cell for the aerial line transect dataset. We used subjective weather condition
187 recorded by plane observers during the line transect protocols as a discrete variable ranging
188 from 1 to 8. Good weather condition was expected to be positively related to the detection
189 probability.

190 **Spatial integrated models for closed populations**

191 To integrate DS and SCR data, we used the hierarchical model proposed by Chandler et
192 al. (2018). However, while initially developed for open populations and due to the lack of
193 temporal depth in our datasets, we adapted the model to estimate abundance and density without
194 accounting for demographic parameters (Fig 1). We performed closed population estimation of
195 bottlenose dolphin density over the 2011-2015 period, assuming that (1) the population was
196 demographically closed during the study period, (2) all individuals were correctly identified at
197 each capture occasion and marks were permanent during the sampling period, (3) no migratory
198 events occurred during the sampling period. Although being strong assumptions, bottlenose
199 dolphin deaths and recruitments between 2011 and 2015 were likely small considering the long
200 life cycle of bottlenose dolphins (Bearzi, Fortuna, & Reeves, 2009; Hammond et al., 2021).
201 Besides, Western Mediterranean bottlenose dolphin population is clustered into coastal
202 subunits, hence we neglected migration events and movements that can occur between “French”
203 resident groups and other populations, e.g. offshore, Spanish, Italian or Atlantic groups (Louis
204 et al., 2014; Carnabuci et al., 2016).

205 We structure our integrated spatial model around two layers with i) an ecological model that
206 describes the density of individuals based on an inhomogeneous point process (*Spatial*
207 *abundance* section below), and ii) two observation models that describe how the DS and SCR
208 data arise from the latent ecological model (*Capture-recapture data* and *Distance-sampling*
209 *data* sections below).

210 **Spatial abundance**

211 For the ecological model, we use a latent spatial point process modelling the density of
212 individuals and the overall abundance. Over the study area S , an intensity function returns the
213 expected number of individuals at location s in S . Here, s , represents an arbitrary point in the
214 study area S . To account for spatial variation, we model the latent density surface as an
215 inhomogeneous point process. For every location s in the study area S , the expected abundance
216 λ is written as a log-linear function of an environmental covariate, say habitat:

$$\log(\lambda(s)) = \mu_0 + \mu_1 \text{habitat}(s) \quad (1)$$

217 where parameters to be estimated are μ_0 and μ_1 respectively the density intercept and the
218 regression coefficient of the environmental covariate. For simplicity, we use depth as a habitat
219 covariate possibly influencing bottlenose dolphin density, and explore a linear relationship
220 between density and depth. The effect of habitat covariates could be further explored (e.g. by
221 considering other covariates such as sea surface temperature or prey availability, or by
222 accounting for non-linear effects). Then, the estimated population size is derived by integrating
223 the intensity function over the study area:

$$E(N) = \int_S \lambda(s) ds. \quad (2)$$

224 As we discretized the study area, we estimated λ_j the intensity process describing density for
225 each grid-cell j with $j = 1, \dots, J = 4356$, hence $E(N) = \sum_{j=1}^J \lambda_j$. The latent ecological process
226 defined by Eq. 1 is an inhomogeneous point process that is common to both the SCR and DS

227 models. SCR and DS data are linked to density λ and informed the parameters of Eq. 1. To
228 account for unseen individuals, we used the data augmentation technique and augmented the
229 observed datasets to reach $M = 20,000$ individuals (Royle & Dorazio, 2012). Each individual i
230 is considered being ($z_i = 1$) or not ($z_i = 0$) a member of the population according to a draw in a
231 Bernoulli distribution of probability ψ , with $z_i \sim \text{Bernoulli}(\psi)$ where ψ is the probability for
232 individual i to be a member of the population, with $\psi = E(N)/M$ and $N = \sum_{i=1}^M z_i$.

233 **Capture-recapture data**

234 To link capture-recapture data with the ecological process, we built a SCR model (Royle et al.,
235 2014). Detection history of individuals were collected over $T = 8$ sampling occasions and
236 capture locations were recorded. Grid-cells j in which sampling effort was positive during an
237 occasion were considered as active detectors for this sampling occasion, hence reflecting that
238 animals could be observed. We stored observations in a three-dimensional array y with y_{ijt}
239 indicating whether individual i was captured at grid-cell j during sampling occasion t . We
240 assume that observation y_{ijt} is an outcome from a Bernoulli distribution with capture probability
241 p_{ijt} , $y_{ijt} \sim \text{Bernoulli}(p_{ijt} z_i)$. We model capture probability with a half-normal detection
242 function $p_{ijt} = p_0 \exp\left(-\frac{d_{ij}^2}{2\sigma_{SCR}^2}\right)$ where d_{ij} is the Euclidian distance between the activity center
243 of individual i and the grid-cell j , σ_{SCR} is the scale parameter of the half-normal function, and
244 p_0 is the baseline encounter rate (Royle et al., 2014). We accounted for spatial and temporal
245 variation in the detection probability through the baseline detection rate p_0 that we modelled as
246 a logit-linear function: $\text{logit}(p_{0,ijt}) = \delta_0 + \delta_1 E_{j,t}$. When the sampling effort $E_{j,t}$ is null, we fixed
247 $p_{0,ijt}$ to 0.

248 The locations of activity center inform the density of individuals λ . For each individual i
249 belonging to the sampled population, its activity center is assigned as the result of a multinomial
250 draw in the predicted density in each grid-cell of the study area.

251 $id_i \sim \text{Multinomial}(1, \bar{\lambda})$

252 where id_i is the activity center of individual i , and $\bar{\lambda}$ represent the vector of the predicted density
253 in each cell of the study area. Due to the computational burden to sample the 4356 grid-cells,
254 we mimicked the multinomial distribution through the “zeros trick” (see R codes for details).
255 We considered that activity centers did not change between sampling occasions.

256 **Distance-sampling data**

257 To accommodate distance data, we built a hierarchical DS model (Kéry & Royle, 2016). We
258 model the DS data conditional on the underlying density surface defined by Eqs (1) and (2).
259 We considered two sampling occasions t_{ds} as some transects were replicated. We assume that
260 the probability of detecting dolphins is a decreasing function of the perpendicular distance
261 between the transect and dolphin group. Because distance may not be estimated with perfection
262 by observers, we discretized the distance of observation in B distance bins. Then, $r_{jbt} =$
263 $r_{0(j,t)} \exp(-\frac{d_b^2}{2\eta^2})$, where η is the scale parameter of the half-normal function, and $r_{0(j)}$ is the
264 probability of detection in the grid-cell j , and d_b is the observation distance between the flight
265 transect and bin b where the detection occurred. The distance class d_j of the observed data at
266 grid-cell j is modelled as a multinomial/categorical draw

267 $d_{j,t} | n_{j,t} \sim \text{Multinomial}(1, \pi_{j,t})$

268 with $\pi_{j,t}$ the vector of length B storing the detection probabilities in each bin b at grid-cell j . The
269 b^{th} index being $\pi_{j,b,t} = r_{j,b,t} / (\sum_b r_{j,b,t})$.

270 We account for spatial variation in the baseline detection rate of the detection function
271 modelling $r_{0(j,t)}$ as a log-linear function of weather condition $W_{j,t}$ in grid-cell j during sampling
272 occasion t :

273 $\text{logit}(r_{0(j,t)}) = \alpha_0 + \alpha_1 W_{j,t}.$

274 Besides, aerial surveys only sampled a fraction of the total area of each grid-cell (Appendix 1).
275 We calculated $S_{j,t}$ the proportion of the grid-cell effectively sampled by aerial surveys
276 considering a 1200 m wide annulus around the transect. We assumed that density within each
277 grid-cell was uniform and remained constant across the sampling period. Then, $N_{j,t}$ the number
278 of individuals sampled by aerial surveys in each grid-cell j during sampling occasion t is
279 Poisson distributed with λ_j being the density of individuals predicted by the point process in
280 grid-cell j restricted to the proportion of grid-cell sampled, $S_{j,t}$.

281
$$N_{j,t} \sim Poisson(\lambda_j S_{j,t})$$

282 Then, $n_{j,t}$ the observed group size detected at grid-cell j during sampling occasion t , is given by
283 a Binomial draw in the expected number of sampled individuals, $N_{j,t}$ with probability the sum
284 of $r_{j,b,t}$, the detection probabilities within each bin b of grid-cell j during sampling occasion t .

285
$$n_{j,t} | N_{j,t} \sim Binomial(N_{j,t}, \sum_b r_{j,b,t})$$

286 Bayesian implementation

287 To highlight the benefit of integrating data for the estimation of bottlenose dolphin
288 density, we compared i) the output of the spatial DS model, ii) the SCR model, and iii) the
289 integrated spatial model.

290 We ran all models with three Markov Chain Monte Carlo chains with 100,000 iterations
291 each in the NIMBLE R package (de Valpine et al., 2017). We checked for convergence
292 calculating the R -hat parameter (Gelman et al., 2013) and reported posterior mean and 80%
293 credible intervals (CI) for each parameter. We considered as important the effect of a regression
294 parameter whenever the 80% CI of its posterior distribution did not include 0. We also
295 calculated the predicted density of bottlenose dolphins (i.e. λ). Data and codes are available on
296 GitHub (<https://github.com/valentinlauret/SpatialIntegratedModelTursiops>).

297 RESULTS

298 We detected 536 dolphins through aerial surveys clustered in 129 groups. We identified
299 927 dolphins over 1707 detections in photo-identification surveys, out of which 638 dolphins
300 were captured only once (68%), 144 were captured twice (15.5%), 149 were captured 3 times
301 and up to 8 times for one individual. The maximum distance between two sightings of the same
302 individual was 302 km, with one individual detected twice during the same sampling occasion
303 at 115 km distance.

304 We estimated 2451 dolphins (2337; 2566) with integrated spatial model over the study
305 area (Table 1), 11531 dolphins (10132; 12997) with the DS model and 1834 dolphins (1745;
306 1926) with the SCR model (Table 1). Density intercepts of integrated spatial model ($\mu_0 = -0.85$
307 (-0.90; -0.79)) and SCR model ($\mu_0 = -1.18$ (-1.81; -1.07)) were lower than intercept of DS model
308 ($\mu_0 = 0.95$ (0.82; 1.08)).

309 DS model estimated a positive effect of shallow waters ($\mu_1 = 0.18$ (0.12; 0.25), Table 1)
310 similar to the effect estimated by the integrated spatial model ($\mu_1 = 0.32$ (0.26; 0.38), Table 1).
311 However, the SCR model did not detect an effect of depth on density ($\mu_1 = 0.28$ (-0.47; 1.22),
312 Table 1). Then, both integrated and DS models predicted higher densities of bottlenose dolphins
313 in the coastal seas than in the pelagic seas, whereas the SCR model predicted no effect of depth
314 on dolphin density.

315 Boat sampling effort exhibited a positive effect on detection probability for both the
316 SCR model ($\beta_1 = 0.58$ (0.53; 0.62)) and the integrated spatial model ($\beta_1 = 0.58$ (0.54; 0.62), table
317 1). For the integrated spatial model and the DS model, the detection probability increased when
318 the weather condition improved (integrated spatial model: $\alpha_1 = 1.64$ (1.15; 2.10), DS: $\alpha_1 = 1.86$
319 (1.52; 2.21), Table 1).

320 **DISCUSSION**

321 **Integrated spatial model benefits from both distance sampling and capture-recapture**
322 **data**

323 With our integrated spatial model, we estimated bottlenose dolphin abundance within the
324 range of what was found in previous studies in nearby areas (Gnone et al., 2011; Lauriano et
325 al., 2014), and found that densities were more likely to be higher in coastal areas (Bearzi,
326 Fortuna, & Reeves, 2009). A striking result was the higher abundance estimated by DS
327 compared to abundance estimated by the integrated and SCR models, which estimates were
328 also found in previous studies analysing the same datasets in isolation. Using CR data only,
329 Labach et al. (2021) estimated 2350 dolphins (95% confidence interval: 1827; 3135) inhabiting
330 the French continental coast where our integrated model predicted 2451 dolphins (95%
331 confidence interval: 2306; 2602). Analysing DS data, Laran et al., (2017) estimated 2946
332 individuals (95% confidence interval: 796; 11,462) during summer, and 10,233 (95%
333 confidence interval: 4217; 24,861) during winter where our DS model estimated 11,531 (95%
334 confidence interval: 9784; 13,478) all year long. Recent aerial campaigns performed in 2018-
335 2019 on the same study area and following the same distance sampling protocol do not suggest
336 seasonal difference in bottlenose dolphins abundance (Laran et al., 2021).

337 We see several reasons that might explain the discrepancy in estimates obtained from SCR
338 and DS models. First, although the Mediterranean bottlenose dolphins population is clustered
339 in coastal sub-units (Carnabuci et al., 2016), groups can be encountered offshore (Bearzi,
340 Fortuna, & Reeves, 2009). In the DS dataset, large dolphin groups were detected in the pelagic
341 seas at the extreme south of sampling design (Appendix 1). These groups could either be i)
342 occasional pelagic individuals belonging to coastal populations and that are mainly resident
343 outside our study area (e.g. Balearic, South-Western Sardinia), or ii) resident pelagic
344 populations that are not sampled by coastal photo-id surveys (Louis et al., 2014). Second, SCR
345 data were restricted to the French continental coast and did not sample dolphin populations that
346 exist elsewhere in the study area, e.g. in Corsica, Liguria, and Tuscany (Carnabuci et al., 2016).
347 Despite this geographic sampling bias in the capture-recapture data, SCR models should predict

348 the existence of Corsican and Italian populations if the relationship between density and habitat
349 in Eq (1) was correct and consistent throughout the study area. Predicting abundance outside
350 the range of the data used could lead to biased estimates if the habitat-density relation is not
351 correctly specified (A. Lee-Yaw et al., 2021; Hammond et al., 2021). As the photo-id surveys
352 did not sample greater depths, our SCR model is likely to underestimate abundance because the
353 relation linking dolphin density to depth was not correctly specified. Thus, we emphasized the
354 relevance of aerial surveys that collected data in the pelagic seas, which helps to quantify the
355 habitat-density relationship. To perform detailed analysis of the NW Mediterranean bottlenose
356 dolphin populations, one should consider additional environmental covariates to better capture
357 spatial variation in density (e.g., sea surface temperature, distance to coast, or 200m contour,
358 Lambert et al. 2017). Besides, because Sardinian and Balearic populations, and offshore groups
359 can be sampled in the aerial surveys, the DS model drives upward abundance compared to the
360 SCR model that is unlikely to account for animals that are members of the Southern neither the
361 Eastern or offshore populations.

362 Overall, both DS and SCR data affected the estimates of the integrated spatial model. Using
363 SCR data brought more information about population size (e.g. more detections, more
364 individuals) than the DS data to inform the intercept of density (μ_0), making the integrated
365 spatial model abundance estimate closer to the SCR model estimate (Table 1, Fig. 2). However,
366 the DS data that were collected throughout the range of the habitat predictor informed the slope
367 of the inhomogeneous point process (μ_1), i.e. the effect of depth on dolphin density. Then, in
368 the integrated spatial model, the SCR data informed the estimated population size and the DS
369 data informed spatial repartition of individuals by correcting for the geographic sampling bias
370 in the SCR data. The integrating approach helped to reduce the sampling limitations of each
371 dataset and can improve the ecological inference as illustrated here about bottlenose dolphins.

372 **Conservation implications for monitoring bottlenose dolphins in the French**

373 **Mediterranean Sea and beyond**

374 When the conservation goal is to assess abundance in an area at a specific time, line transect
375 surveys may be a cost-effective choice. However, if one's goal is to estimate the number of
376 animals in an area over a longer period, CR methods could be more appropriate but have cost
377 implications that may exceed those of conducting a line transect survey (Crum, Neyman, &
378 Gowan, 2021; Hammond et al., 2021). Despite differences in ecological inference, DS and CR
379 are complementary methods depending on the conservation motivations and funding. To date,
380 assessing bottlenose dolphin population of French Mediterranean Sea for the EU reporting only
381 focuses on the DS data (Laran et al., 2017). Aerial surveys provide crucial information on
382 marine megafauna taxa, and on human pressures to fill several criteria of the Marine Strategy
383 Framework Directive (Laran et al., 2017; Pettex et al., 2017; Lambert et al., 2020). However,
384 funding constraints make the aerial monitoring hardly applicable at a high frequency, and it is
385 planned to be implemented every 6 years. In parallel, the French office for biodiversity develops
386 and supports local monitoring programs in the French MPA network to perform photo-id data
387 continuously, such detailed datasets represent an important asset to inform abundance of marine
388 mammals populations (Evans & Hammond, 2004). Ecological indicators required by the
389 Marine Strategy Framework Directive for bottlenose dolphins would benefit from integrating
390 aerial line-transect with more data when available (Lauret et al. 2021). In addition, the French
391 Research Institute for Exploitation of the Sea (i.e. IFREMER) collected yearly bottlenose
392 dolphins' data during line transects surveys for pelagic fisheries (Baudrier et al., 2018).
393 Ultimately, several monitoring programs will be available about bottlenose dolphins in the
394 Mediterranean context and integrated spatial models makes possible to include existing datasets
395 that have been discarded so far to inform public policies (Cheney et al., 2013; Isaac et al., 2019).

396 We acknowledge that our model has limitations due to several ecological features lacking, e.g.
397 spatial autocorrelation, effect of other environmental covariates, accounting for non-linear
398 covariate effect, and group behaviour of bottlenose dolphins that may generate non-independent
399 individual detection probabilities. One might also consider extending the activity center process
400 to include a movement model of individuals (Gowan, Crum, & Roberts, 2021). Moreover,
401 ecological closure assumptions we assumed are likely to be violated but we assumed the bias
402 introduced bias would be minimal. However, we emphasize that integrated spatial models are
403 highly relevant considering the future monitoring planning by the French biodiversity agency
404 that will perpetuate the coexistence of photo-identification with aerial line-transect. Analysing
405 the collected data in an integrated framework will lead to a more comprehensive understanding
406 of how the monitoring programs can work together and what exactly it is that they achieve in
407 unison. It is our hope that the ability of integrating different datasets contribute to the ongoing
408 monitoring efforts developed in the Mediterranean context and fit in the scope of what
409 managers expect from statistical developments to inform environmental policies (Lauret, 2021).

410 Line-transect and capture-recapture surveys are widely used monitoring methods to assess
411 population dynamics of marine mammals (Hammond et al., 2021). Our work provides a
412 promising modelling baseline to deal with the bottlenose dolphin evaluation but also open
413 perspectives for other conservation challenges about marine species that are subject to similar
414 monitoring situations in the French Mediterranean context (e.g. fin whale, seabirds) and
415 elsewhere.

416 Last, adding complementary long-term datasets to the aerial-surveys would make possible
417 to access the demographic parameters (e.g. recruitments, survival (Chandler et al. 2018)), which
418 would represent a major opportunity for the knowledge about French Mediterranean bottlenose
419 dolphin populations and to produce reliable conservation status. The use of integrated spatial
420 models for the French Mediterranean bottlenose dolphin population also enable to extend the

421 modelling approach exploring seasonality in density, and to measure immigration and dispersal
422 between bottlenose dolphins populations (Zipkin & Saunders, 2018). Finally, precising the
423 assessment of bottlenose dolphin conservation status could ultimately lead to mitigation
424 programs in the context of the Marine Strategy Framework Directive, e.g. marine protected
425 areas implementation such as the Bottlenose dolphins Natura 2000 area in the French Gulf of
426 Lion.

427 **Spatial integrated models as a promising tool for conservation**

428 When establishing species conservation status for large-scale environmental policies,
429 discarding some datasets from the analysis can reduce the reliability of the ecological estimation
430 (Bischof, Brøseth, & Gimenez, 2016). Using multiple datasets into integrated spatial models
431 help to overcome some limitations present when using separated information sources (e.g.
432 limited spatial or temporal survey coverage, Zipkin & Saunders 2018; Isaac et al. 2019).
433 However, caution should be taken as integrating data requires additional modelling
434 assumptions, e.g. assuming population closure over longer time period in our case (Dupont et
435 al., 2019; Farr et al., 2020; Fletcher et al., 2019; Simmonds et al., 2020). Integrated spatial
436 models are flexible tools that can include more than 2 datasets (Zipkin & Saunders, 2018), and
437 various type of data that enlarge the scope of usable information (presence-absence (Santika et
438 al. 2017), count data (Chandler et al., 2018), citizen science data (Sun, Royle, & Fuller, 2019)).
439 Recent and current developments of SCR models widen perspectives to extend integrated
440 spatial models to account for unidentified individuals, or to better describe animal movement
441 (Milleret et al., 2019; Jiménez et al., 2020; Turek et al., 2020). Over the last decades, the spatial
442 scope of conservation efforts has greatly increased, and the analytical methods have had to
443 adapt accordingly (Zipkin & Saunders, 2018). Integrated spatial models are a promising tool
444 that can be used in multiple situations where several data sources coexist, especially for large
445 scale conservation policies.

446 ACKNOWLEDGEMENTS

447 The French Ministry in charge of the environment (Ministère de la Transition Energetique et
448 Solidaire) and the French Office for Biodiversity (OFB) funded the project SAMM that
449 performed the aerial line-transects. The PELAGIS observatory, with the help of the OFB,
450 designed, coordinated and conducted the survey: Emeline Pettex, Ghislain Doremus and Olivier
451 Van Canneyt. We thank all the observers: Léa David (cruise leader), Eric Stéphan (cruise
452 leader), Thomas Barreau, Ariane Blanchard, Vincent Bretille, Alexis Chevalier, Cécile Dars,
453 Olivier Dian, Nathalie Di-Méglion, Emilie Durand, Marc Duvilla, Emmanuel Levesque,
454 Alessio Maglio, Marie Pellé, Morgane Perri, and Sandrine Serre. We are indebted to all aircraft
455 crew members of Pixair Survey and the logistic partnership SINAY. We are grateful to all
456 financial partners of the GDEGeM project that performed the photo-identification monitoring.
457 We warmly thank technical and scientific participants of GDEGeM.

458 LITTERATURE CITED

459 A. Lee-Yaw, J., L. McCune, J., Pironon, S., & N. Sheth, S. (2021). Species distribution models rarely
460 predict the biology of real populations. *Ecography* **44**, 1–16.
461 Authier, M., Commanducci, F. D., Genov, T., Holcer, D., Ridoux, V., Salivas, M., Santos, M. B., &
462 Spitz, J. (2017). Cetacean conservation in the Mediterranean and Black Seas: Fostering
463 transboundary collaboration through the European Marine Strategy Framework Directive.
464 *Mar. Policy* **82**, 98–103.
465 Baudrier, J., Lefebvre, A., Galgani, F., Saraux, C., & Doray, M. (2018). Optimising French fisheries
466 surveys for marine strategy framework directive integrated ecosystem monitoring. *Mar. Policy*
467 **94**, 10–19.
468 Bearzi, G., Fortuna, C. M., & Reeves, R. R. (2009). Ecology and conservation of common bottlenose
469 dolphins *Tursiops truncatus* in the Mediterranean Sea. *Mammal Rev.* **39**, 92–123.
470 Besbeas, P., Freeman, S. N., Morgan, B. J., & Catchpole, E. A. (2002). Integrating mark–recapture–
471 recovery and census data to estimate animal abundance and demographic parameters.
472 *Biometrics* **58**, 540–547.
473 Bischof, R., Brøseth, H., & Gimenez, O. (2016). Wildlife in a Politically Divided World: Insularism
474 Inflates Estimates of Brown Bear Abundance: Transboundary wildlife populations. *Conserv.*
475 *Lett.* **9**, 122–130.
476 Bischof, R., Milleret, C., Dupont, P., Chipperfield, J., Tourani, M., Ordiz, A., de Valpine, P., Turek,
477 D., Royle, J. A., Gimenez, O., Flagstad, Ø., Åkesson, M., Svensson, L., Brøseth, H., &
478 Kindberg, J. (2020). Estimating and forecasting spatial population dynamics of apex predators
479 using transnational genetic monitoring. *Proc. Natl. Acad. Sci.* **117**, 30531–30538.
480 Buckland, Magurran, A. E., Green, R. E., & Fewster, R. M. (2005). Monitoring change in biodiversity
481 through composite indices. *Philos. Trans. R. Soc. B Biol. Sci.* **360**, 243–254.
482 Buckland, S. T., Anderson, D. R., Burnham, K. P., & Laake, J. L. (2005). Distance sampling. *Encycl.*

483 *Biostat. 2.*

484 Calambokidis, J., & Barlow, J. (2004). Abundance of blue and humpback whales in the eastern north
485 pacific estimated by capture-recapture and line-transect methods. *Mar. Mammal Sci.* **20**, 63–
486 85.

487 Camp, R. J., Miller, D. L., Thomas, L., Buckland, S. T., & Kendall, S. J. (2020). Using density surface
488 models to estimate spatio-temporal changes in population densities and trend. *Ecography*.

489 Carnabuci, M., Schiavon, G., Bellingeri, M., Fossa, F., Paoli, C., Vassallo, P., & Gnane, G. (2016).
490 Connectivity in the network macrostructure of *Tursiops truncatus* in the Pelagos Sanctuary
491 (NW Mediterranean Sea): does landscape matter? *Popul. Ecol.* **58**, 249–264.

492 Chandler, R. B., & Clark, J. D. (2014). Spatially explicit integrated population models. (E. Cooch,
493 Ed.)*Methods Ecol. Evol.* **5**, 1351–1360.

494 Chandler, R. B., Hepinstall-Cymerman, J., Merker, S., Abernathy-Conners, H., & Cooper, R. J.
495 (2018). Characterizing spatio-temporal variation in survival and recruitment with integrated
496 population models. *The Auk* **135**, 409–426.

497 Cheney, B., Thompson, P. M., Ingram, S. N., Hammond, P. S., Stevick, P. T., Durban, J. W., Culloch,
498 R. M., Elwen, S. H., Mandleberg, L., Janik, V. M., Quick, N. J., ISLAS-Villanueva, V.,
499 Robinson, K. P., Costa, M., Eisfeld, S. M., Walters, A., Phillips, C., Weir, C. R., Evans, P. G.
500 H., Anderwald, P., Reid, R. J., Reid, J. B., & Wilson, B. (2013). Integrating multiple data
501 sources to assess the distribution and abundance of bottlenose dolphins *Tursiops truncatus* in
502 Scottish waters: Abundance of bottlenose dolphins around Scotland. *Mammal Rev.* **43**, 71–88.

503 Council Directive 92/43/EEC of 21 May 1992 on the conservation of natural habitats and of wild
504 fauna and flora. , OJ L 206 (1992).

505 Crum, N. J., Neyman, L. C., & Gowan, T. A. (2021). Abundance estimation for line transect sampling:
506 A comparison of distance sampling and spatial capture-recapture models. *PLOS ONE* **16**,
507 e0252231.

508 de Valpine, P., Turek, D., Paciorek, C. J., Anderson-Bergman, C., Lang, D. T., & Bodik, R. (2017).
509 Programming with models: writing statistical algorithms for general model structures with
510 NIMBLE. *J. Comput. Graph. Stat.* **26**, 403–413.

511 Directive 2008/56/EC of the European Parliament and of the Council of 17 June 2008 establishing a
512 framework for community action in the field of marine environmental policy (Marine Strategy
513 Framework Directive) (Text with EEA relevance). , OJ L 164 (2008).

514 Dupont, P., Milleret, C., Gimenez, O., & Bischof, R. (2019). Population closure and the bias-precision
515 trade-off in spatial capture–recapture. (M. Auger-Méthé, Ed.)*Methods Ecol. Evol.* **10**, 661–
516 672.

517 Evans, P. G. H., & Hammond, P. S. (2004). Monitoring cetaceans in European waters. *Mammal Rev.*
518 **34**, 131–156.

519 Farr, M. T., Green, D. S., Holekamp, K. E., & Zipkin, E. F. (2020). Integrating distance sampling and
520 presence-only data to estimate species abundance. *Ecology*.

521 Fletcher, R. J., Hefley, T. J., Robertson, E. P., Zuckerberg, B., McCleery, R. A., & Dorazio, R. M.
522 (2019). A practical guide for combining data to model species distributions. *Ecology* e02710.

523 Gelman, A., Carlin, J. B., Stern, H. S., Dunson, D. B., Vehtari, A., & Rubin, D. B. (2013). Bayesian
524 data analysis. Chapman and Hall/CRC.

525 Gnane, G., Bellingeri, M., Dhermain, F., Dupraz, F., Nuti, S., Bedocchi, D., Moulins, A., Rosso, M.,
526 Alessi, J., McCrea, R. S., Azzellino, A., Airolidi, S., Portunato, N., Laran, S., David, L., Di
527 Meglio, N., Bonelli, P., Montesi, G., Trucchi, R., Fossa, F., & Wurtz, M. (2011). Distribution,
528 abundance, and movements of the bottlenose dolphin (*Tursiops truncatus*) in the Pelagos
529 Sanctuary MPA (north-west Mediterranean Sea): THE BOTTLENOSE DOLPHIN IN THE
530 PELAGOS SANCTUARY MPA. *Aquat. Conserv. Mar. Freshw. Ecosyst.* **21**, 372–388.

531 Gowan, T. A., Crum, N. J., & Roberts, J. J. (2021). An open spatial capture–recapture model for
532 estimating density, movement, and population dynamics from line-transect surveys. *Ecol.
533 Evol.* **11**, 7354–7365.

534 Hammond, P. S., Francis, T. B., Heinemann, D., Long, K. J., Moore, J. E., Punt, A. E., Reeves, R. R.,
535 Sepúlveda, M., Sigurðsson, G. M., Siple, M. C., Víkingsson, G., Wade, P. R., Williams, R., &
536 Zerbini, A. N. (2021). Estimating the Abundance of Marine Mammal Populations. *Front. Mar.
537 Sci.* **8**, 735770.

538 Isaac, N. J. B., Jarzyna, M. A., Keil, P., Dambly, L. I., Boersch-Supan, P. H., Browning, E., Freeman,
539 S. N., Golding, N., Guillera-Arroita, G., Henrys, P. A., Jarvis, S., Lahoz-Monfort, J., Pagel, J.,
540 Pescott, O. L., Schmucki, R., Simmonds, E. G., & O'Hara, R. B. (2019). Data Integration for
541 Large-Scale Models of Species Distributions. *Trends Ecol. Evol.*

542 IUCN. (2009, November 18). *Tursiops truncatus* (Mediterranean subpopulation): Bearzi, G., Fortuna,
543 C. & Reeves, R.: The IUCN Red List of Threatened Species 2012: e.T16369383A16369386.
544 International Union for Conservation of Nature.

545 Jiménez, J., Augustine, B., Linden, D. W., Chandler, R., & Royle, J. A. (2020). Spatial capture–
546 recapture with random thinning for unidentified encounters. *Ecol. Evol.* ece3.7091.

547 Kéry, M., & Royle, J. (2020). Applied hierarchical modeling in ecology: analysis of distribution,
548 abundance and species richness in r and bugs: volume 2: dynamic and advanced models. 1st
549 ed., Vol. Ch 10. Cambridge: Elsevier.

550 Kéry, M., & Royle, J. A. (2016). Applied hierarchical modeling in ecology: analysis of distribution,
551 abundance and species richness in R and BUGS. Amsterdam ; Boston: Elsevier/AP, Academic
552 Press is an imprint of Elsevier.

553 Labach, H., Azzinari, C., Barbier, M., Cesarini, C., Daniel, B., David, L., Dhermain, F., Di-Méglie,
554 N., Guichard, B., Jourdan, J., Lauret, V., Robert, N., Roul, M., Tomasi, N., & Gimenez, O.
555 (2021). Distribution and abundance of common bottlenose dolphin (*Tursiops truncatus*) over
556 the French Mediterranean continental shelf. *Mar. Mammal Sci.* n/a.

557 Labach, H., Azzinari, C., Barbier, M., Cesarini, C., Daniel, B., David, L., Dhermain, F., Di-Méglie,
558 N., Guichard, B., Jourdan, J., Robert, N., Roul, M., Tomasi, N., & Gimenez, O. (2019).
559 Distribution and abundance of bottlenose dolphin over the French Mediterranean continental
560 shelf. *bioRxiv*.

561 Lambert, C., Authier, M., Dorémus, G., Laran, S., Panigada, S., Spitz, J., Van Canneyt, O., & Ridoux,
562 V. (2020). Setting the scene for Mediterranean litterscape management: The first basin-scale
563 quantification and mapping of floating marine debris. *Environ. Pollut.* **263**, 114430.

564 Lambert, C., Virgili, A., Pettex, E., Delavenne, J., Toison, V., Blanck, A., & Ridoux, V. (2017).
565 Habitat modelling predictions highlight seasonal relevance of Marine Protected Areas for
566 marine megafauna. *Deep Sea Res. Part II Top. Stud. Oceanogr.* **141**, 262–274.

567 Laran, S., Nivière, M., Dorémus, G., Serre, S., Spitz, J., & Authier, M. (2021). Distribution et
568 abondance de la mégafaune marine lors des campagnes SAMM cycle I et II en Méditerranée
569 78.

570 Laran, S., Pettex, E., Authier, M., Blanck, A., David, L., Dorémus, G., Falchetto, H., Monestiez, P.,
571 Van Canneyt, O., & Ridoux, V. (2017). Seasonal distribution and abundance of cetaceans
572 within French waters- Part I: The North-Western Mediterranean, including the Pelagos
573 sanctuary. *Deep Sea Res. Part II Top. Stud. Oceanogr.* **141**, 20–30.

574 Lauret, V. (2021, October 21). Étudier les suivis écologiques dans les Aires Marines Protégées de
575 Méditerranée française : une approche interdisciplinaire autour du grand dauphin (phdthesis).
576 Université Montpellier.

577 Lauret, V., Labach, H., Authier, M., & Gimenez, O. (2021). Using single visits into integrated
578 occupancy models to make the most of existing monitoring programs. *Ecology* 848663.

579 Lauriano, G., Pierantonio, N., Donovan, G., & Panigada, S. (2014). Abundance and distribution of
580 *Tursiops truncatus* in the Western Mediterranean Sea: An assessment towards the Marine
581 Strategy Framework Directive requirements. *Mar. Environ. Res.* **100**, 86–93.

582 Lindenmayer, D. B., & Likens, G. E. (2010). The science and application of ecological monitoring.
583 *Biol. Conserv.* **143**, 1317–1328.

584 Louis, M., Fontaine, M. C., Spitz, J., Schlund, E., Dabin, W., Deaville, R., Caurant, F., Cherel, Y.,
585 Guinet, C., & Simon-Bouhet, B. (2014). Ecological opportunities and specializations shaped
586 genetic divergence in a highly mobile marine top predator. *Proc. R. Soc. B Biol. Sci.* **281**,
587 20141558.

588 Miller, D. A. W., Pacifici, K., Sanderlin, J. S., & Reich, B. J. (2019). The recent past and promising
589 future for data integration methods to estimate species' distributions. (B. Gardner,
590 Ed.)*Methods Ecol. Evol.* **10**, 22–37.

591 Miller, D. L., Burt, M. L., Rexstad, E. A., & Thomas, L. (2013). Spatial models for distance sampling
592 data: recent developments and future directions. (O. Gimenez, Ed.)*Methods Ecol. Evol.* **4**,

593 1001–1010.

594 Milleret, C., Dupont, P., Bonenfant, C., Brøseth, H., Flagstad, Ø., Sutherland, C., & Bischof, R.
595 (2019). A local evaluation of the individual state-space to scale up Bayesian spatial capture–
596 recapture. *Ecol. Evol.* **9**, 352–363.

597 Nichols, & Williams. (2006). Monitoring for conservation. *Trends Ecol. Evol.* **21**, 668–673.

598 Niemi, G. J., & McDonald, M. E. (2004). Application of Ecological Indicators. *Annu. Rev. Ecol. Evol.
599 Syst.* **35**, 89–111.

600 Pettex, E., David, L., Authier, M., Blanck, A., Dorémus, G., Falchetto, H., Laran, S., Monestiez, P.,
601 Van Canneyt, O., Virgili, A., & Ridoux, V. (2017). Using large scale surveys to investigate
602 seasonal variations in seabird distribution and abundance. Part I: The North Western
603 Mediterranean Sea. *Deep Sea Res. Part II Top. Stud. Oceanogr.* **141**, 74–85.

604 Royle, J. A., Chandler, R. B., Sollmann, R., & Gardner, B. (Eds.). (2014). Spatial capture-recapture.
605 Amsterdam: Elsevier.

606 Royle, J. A., & Dorazio, R. M. (2012). Parameter-expanded data augmentation for Bayesian analysis
607 of capture–recapture models. *J. Ornithol.* **152**, 521–537.

608 Santika, T., Ancrenaz, M., Wilson, K. A., Spehar, S., Abram, N., Banes, G. L., Campbell-Smith, G.,
609 Curran, L., d'Arcy, L., Delgado, R. A., Erman, A., Goossens, B., Hartanto, H., Houghton, M.,
610 Husson, S. J., Kühl, H. S., Lackman, I., Leiman, A., Llano Sanchez, K., Makinuddin, N.,
611 Marshall, A. J., Meididit, A., Mengersen, K., Musnanda, Nardiyono, Nurcahyo, A., Odom, K.,
612 Panda, A., Prasetyo, D., Purnomo, Rafiastanto, A., Raharjo, S., Ratnasari, D., Russon, A. E.,
613 Santana, A. H., Santoso, E., Sapari, I., Sihite, J., Suyoko, A., Tjiu, A., Utami-Atmoko, S. S.,
614 van Schaik, C. P., Voigt, M., Wells, J., Wich, S. A., Willems, E. P., & Meijaard, E. (2017).
615 First integrative trend analysis for a great ape species in Borneo. *Sci. Rep.* **7**, 4839.

616 Schaub, M., & Abadi, F. (2011). Integrated population models: a novel analysis framework for deeper
617 insights into population dynamics. *J. Ornithol.* **152**, 227–237.

618 Simmonds, E. G., Jarvis, S. G., Henrys, P. A., Isaac, N. J. B., & O'Hara, R. B. (2020). Is more data
619 always better? A simulation study of benefits and limitations of integrated distribution models.
620 *Ecography* ecog.05146.

621 Sun, C. C., Royle, J. A., & Fuller, A. K. (2019). Incorporating citizen science data in spatially explicit
622 integrated population models. *Ecology* **100**.

623 Turek, D., Milleret, C., Ergon, T., Brøseth, H., & de Valpine, P. (2020). Efficient Estimation of Large-
624 Scale Spatial Capture-Recapture Models (preprint). *Ecology*.

625 Williams, Nichols, & Conroy. (2002). Analysis and Management of Animal Populations. Academic
626 Press, San Diego, California, USA.

627 Zipkin, E. F., Inouye, B. D., & Beissinger, S. R. (2019). Innovations in data integration for modeling
628 populations. *Ecology* e02713.

629 Zipkin, E. F., & Saunders, S. P. (2018). Synthesizing multiple data types for biological conservation
630 using integrated population models. *Biol. Conserv.* **217**, 240–250.

631

632

TABLES

633 Table 1: Parameter estimates for the spatial integrated model (SIM), spatial capture-recapture (SCR) model, and distance-sampling (DS) model.

634 For each parameter, we display the posterior mean and its 80% credible interval (CI).

Parameter	SIM		SCR model		DS model		635
	Mean	80% CI	Mean	80% CI	Mean	80% CI	
Estimated population size N	2451	2337, 2566	1834	1745, 1926	11531	10132, 12697	636
Intercept of density μ_0	-0.85	-0.90, -0.79	-1.18	-1.81, -1.07	0.95	0.82, 1.038	637
Effect of depth on density μ_1	0.32	0.26, 0.38	0.28	-0.47, 1.22	0.18	0.12, 0.39	638
SCR scale parameter: σ_{SCR}	531	156, 903	2458	500, 5920			640
SCR p_0 parameter: Intercept δ_0	-12.54	-12.93, -12.16	-12.77	-13.53, -12.11			641
SCR p_0 parameter: Effect of at-sea sampling-effort δ_1	0.58	0.54, 0.63	0.58	0.53, 0.62			642
DS scale parameter: σ_{DS}	3.21	1.09, 8.51			4.16	7.14, 9.44	643
DS r_0 parameter: Intercept α_0	3.32	2.80, 3.87			1.15	0.79, 1.51	644
DS r_0 parameter: Effect of weather condition α_1	1.64	1.15 2.1			1.86	1.52, 2.21	645
							646

647

648

649

FIGURE-LEGEND PAGE

650

651 **Figure 1:** Graphical description of the Spatial Integrated Model (SIM) that combines Spatial
652 Capture Recapture (SCR), and Distance Sampling (DS). The SIM is a hierarchical model with
653 three processes: i) latent population size $E(N)$ and density λ informed by an inhomogeneous
654 point process, ii) DS observation process that link the line-transect dataset to the latent density
655 surface, iii) SCR observation process that links the detection histories to the latent density. The
656 observation process is stochastic according to detection probability. For DS model, the
657 observed group size n_{obs} is a Binomial draw in the latent abundance N at the sampl grid-cell.
658 For SCR model, observing an individual i is a Bernoulli draw with a detection probability p_i .
659 Through the data augmentation process with a hypothetical population size M , the probability
660 an individual i belong to the study population is the result of a Bernoulli draw of probability
661 $E(N)/M$.

662

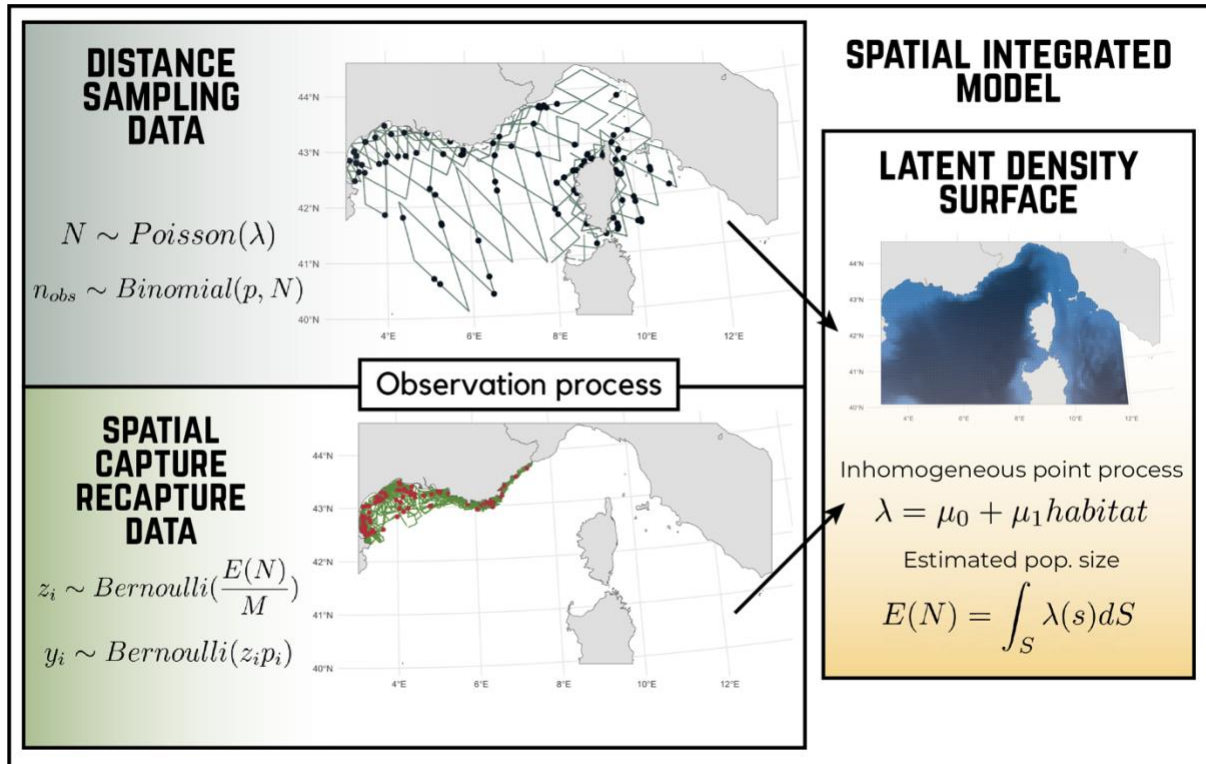
663 **Figure 2:** Estimated density surface of bottlenose dolphins (*Tursiops truncatus*) for the 3
664 models. Lighter colour indicates more individuals per area unit. Both spatial integrated model
665 (SIM) and distance sampling (DS) predicted higher density in coastal seas, while spatial
666 capture-recapture (SCR) predicted homogeneous density across the study area. Note that
667 density scales are different between maps, indicating a higher overall population size for DS
668 model than for SIM, and SCR model.

669

670

671

FIGURES WITH LEGEND

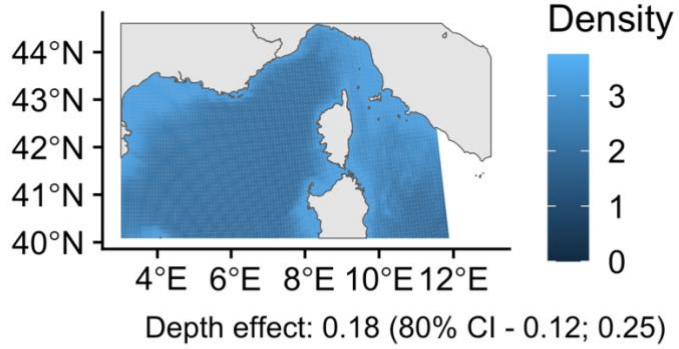


672

673 **Figure 1:** Graphical description of the Spatial Integrated Model (SIM) that combines Spatial
 674 Capture Recapture (SCR), and Distance Sampling (DS). The SIM is a hierarchical model with
 675 three processes: i) latent population size $E(N)$ and density λ informed by an inhomogeneous
 676 point process, ii) DS observation process that link the line-transect dataset to the latent density
 677 surface, iii) SCR observation process that links the detection histories to the latent density. The
 678 observation process is stochastic according to detection probability. For DS model, the
 679 observed group size n_{obs} is a Binomial draw in the latent abundance N at the sampled grid-cell.
 680 For SCR model, observing an individual i is a Bernoulli draw with a detection probability p_i .
 681 Through the data augmentation process with a hypothetical population size M , the probability
 682 an individual i belongs to the study population is the result of a Bernoulli draw of probability
 683 $E(N)/M$.

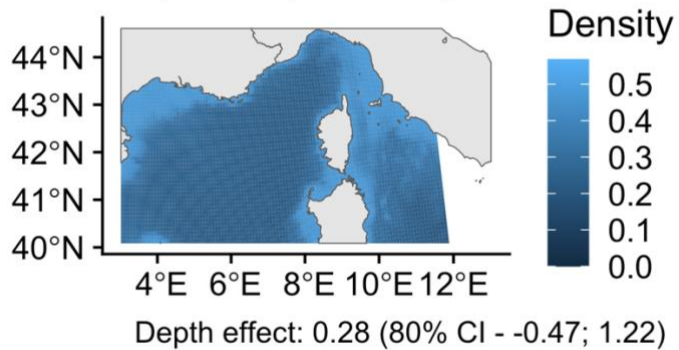
Bottlenose dolphin density

1. Distance Sampling



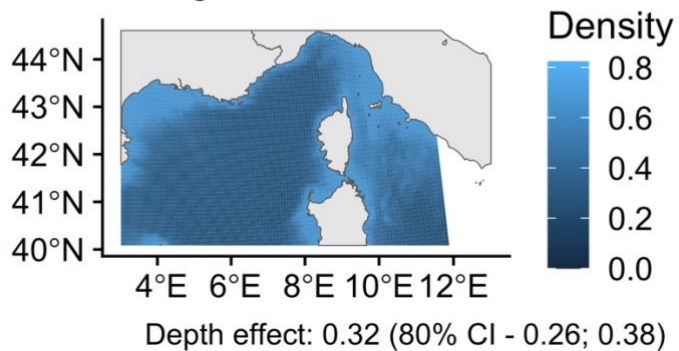
Est. abundance: 11531 (80% CI - 10132; 12997)

2. Spatial Capture Recapture



Est. abundance: 1834 (80% CI - 1745; 1926)

3. Integrated model



Est. abundance: 2451 (80% CI - 2337; 2566)

684

685 **Figure 2: Density of bottlenose dolphins (*Tursiops truncatus*) estimated from 1. Distance**

686 Sampling (DS), 2. Spatial Capture Recapture (SCR), 3. Integrated model. Lighter colour

687 indicates more individuals per area unit. All models predicted higher density in coastal seas,

688 while depth effect is no significant for SCR model. Note that density scales are different

689 between maps, indicating a higher overall population size for DS model than for Integrated

690 model and SCR model.